



Fiber Bragg grating sensors for aerospace applications: a review

Gautam Hegde¹ · S. Asokan¹ · Gopalkrishna Hegde²

Received: 23 January 2022 / Revised: 15 March 2022 / Accepted: 18 March 2022

© Institute of Smart Structures & Systems, Department of Aerospace Engineering, Indian Institute of Science, Bangalore 2022

Abstract

With the advancements in fiber optics, FBG sensors have become one of the most widely used sensors in a diverse range of applications such as civil engineering, telecommunication, biomedical, automotive, aerospace, etc. This is due to their attractive properties of flexibility, lightweight, immunity to electromagnetic interference (EMI), high sensitivity and serial multiplexability. In aerospace engineering-related applications where high precision, remote sensing and lightweight sensors are crucial, FBG sensors have proved to be excellent candidates. In this article, we have provided an overview of the advancements in FBG sensing technology for various applications in the field of aerospace engineering, namely high pressure sensing, ground-based aerodynamic test facilities, shock pressure sensing, spacecraft monitoring and structural health monitoring of aircraft composites.

Keywords FBG sensors · Photosensitivity · Shock pressure · Aerodynamic test facilities · Structural health monitoring

Introduction

The use of optical fibers has grown tremendously in the last 20 years, particularly in the telecommunication sector. There is also a parallel development in exploring and using fiber optic-based sensors for various applications. This has resulted in increased research and improvements in the performance of fiber optic-related components and therefore, a reduction in their cost. Because of their compactness, electrical/chemical inertness and high sensitivity, fiber optic sensors are also being investigated for use in various commercial and industrial applications. There are different types of fiber optic sensors, viz. intensity-based, polarization-based, grating-based, scattering-based sensors, reported in the literature for varieties of applications in aerospace engineering (Di Sante 2015). Among the fiber optic sensors, fiber Bragg grating sensors (FBGs) have been widely used in a variety of applications. FBGs were first fabricated by K.O. Hill et al., at Communications

Research Centre in 1978 in germanosilicate fiber by launching visible Argon ion laser into the fiber. However, interest in FBGs increased with the development of side writing technique by Meltz et al., almost 10 years later. Now, high-quality gratings with precise control over refractive index modulation can be fabricated with several techniques like phase-mask, point-by-point, interferometric, femtosecond laser and draw tower gratings in shorter time duration. FBGs are more attractive compared to other types of fiber optic sensors due to their wavelength encoded sensing nature, which is independent of light source intensity variations, lack of need for bulk optics like mirrors and lenses, high sensitivity, multi-parameter sensing capability and serial multiplexability allowing multipoint sensing with a single fiber. FBG sensors are intrinsically sensitive to strain and temperature, but they have been used to measure a multitude of other parameters like pressure, displacement, acceleration, relative humidity, refractive index, vibration levels. FBG sensors have been used in strain monitoring for damage detection in bridges, buildings, dams, and other civil engineering applications. They have been used in smart manufacturing of composites for aircraft and space structures. FBG sensors have found applications in marine engineering as underwater acoustic sensors, structural health monitoring of ships and submarines. Biomedical applications have also employed FBG sensors due to their chemical passivity, higher sensitivity

✉ Gautam Hegde
gautamhegde@iisc.ac.in

¹ Department of Instrument and Applied Physics, Indian Institute of Science, Bengaluru 560012, India

² BioSystems Science and Engineering, Indian Institute of Science, Bengaluru 560012, India

and diminutive size for pulse monitoring, gait analysis. Etched FBG sensors have been used in chemical sensing for water quality monitoring (Mihailov 2012; Othonos and Kalli 1999; Othonos 1997; Hill et al. 1978, 1993; Meltz et al. 1989; Kashyap 1999; Meltz and Morey 1991).

A variety of sensing diagnostics is required in aerospace applications both in industry and research. Multiple parameters like strain, temperature, pressure, acceleration, vibration, etc., must be monitored while fabrication, testing and onboard missions of aircraft and spacecraft systems. Flow around aircraft test models are simulated in aerodynamic ground test facilities like wind tunnels and shock tunnels. A wide range of sensors are required to gather crucial information about flow parameters as well as aerodynamic parameters around the test model. The type of sensor used depends on the measurand as well as the application. Mechanical-based sensors were used initially but they were found to be less precise, easily affected by external environment like vibrations, electromagnetic interference and are bulky. They were replaced with electrical-based sensors which had faster response, increased repeatability, and higher lifetime. But they do suffer from some disadvantages like danger of electric sparking, electromagnetic interference (EMI) and noise pickup, cumbersome electrical connections, and bulky data acquisition instruments. Fiber optic sensing systems provide a suitable alternative to electrical-based sensors owing to their lightweight, freedom from electric sparking due to their dielectric nature, immunity to EMI, chemical passivity, and flexibility. They can be employed in remote locations in the aircraft structure and used in harsh conditions like explosion environments. FBG sensors can be serially multiplexed with several sensors in a single fiber which increases the sensor capacity. Multi-parameter sensing capability of FBG sensors makes them a perfect candidate for aerospace applications. The lightweight of FBG-based sensing systems is important for space systems as it reduces fuel consumption and increases payload capacity.

In this article, we have attempted to review the recent developments in applications of FBG sensors in different fields of aerospace engineering both in ground-based test facilities and onboard missions of aircraft and spacecraft systems. Before going into real-time onboard missions, most of the systems are tested and evaluated in ground-based test facilities. For example, shock phenomena which are encountered in high-speed flow analysis are an important aspect of research in high-speed aerodynamics. These experiments are generally conducted in shock tunnels and wind tunnels. FBG-based sensing is a promising technique for shockwave studies and is a rapidly developing field. Application of FBG sensors in ground-based aerodynamic test facilities (wind tunnels and shock tunnels), evacuation monitoring, spacecraft applications and

structural health monitoring of aircraft composites have been briefly summarized. Implementation of FBG sensors in such complex experiments and different signal interrogation systems (configurations) developed so far, have also been discussed.

Principle of fiber Bragg grating (FBG) sensors

An FBG is a uniform, periodic modulation of refractive index in the core of a germanium doped (photosensitive) single mode fiber. This modulation of the core effective refractive index can be inscribed using a variety of techniques like Phase mask technique, Interferometric technique and Point-by-Point writing. All the three techniques mainly use UV excimer laser sources. The FBG behaves as an optical filter by reflecting a narrow band of wavelengths, centered around the Bragg wavelength, and is transparent to the remaining wavelengths of an incident broadband light coupled into the fiber as shown in Fig. 1. The Bragg wavelength satisfies the energy and momentum conservation equations, which form the Bragg grating condition. The Bragg wavelength, λ_B , at the center of the reflected spectrum, depends on the effective refractive index of the core n_{eff} , and the spatial interval of the index modulation Λ , called the period of the grating. The Bragg grating condition is written as

$$\lambda_B = 2n_{\text{eff}}\Lambda \quad (1)$$

The effective core refractive index n_{eff} and grating period Λ are sensitive to disturbances in the external environment like strain and temperature. This responsiveness of the Bragg wavelength makes the FBG to function as a sensor. The strain sensitivity of the FBG is due to the strain-optic or the photo-elastic effect i.e., change in core refractive index with strain and compression or elongation of grating period. The Bragg wavelength response to mechanical strain is written as:

$$\frac{\Delta\lambda_B}{\lambda_B} = (1 - \rho_e)\varepsilon \quad (2)$$

where ρ_e is the effective strain-optic coefficient of the fiber core material and ε is the longitudinal strain applied on the fiber. The term ρ_e is a function of the photoelastic constants p_{ij} in the strain optic tensor and the Poisson's ratio ν of the core and is expressed as

$$\rho_e = \frac{n_{\text{eff}}^2}{2} [p_{12} - \nu(p_{11} + p_{12})] \quad (3)$$

For a silica core fiber, n_{eff} is approximately 1.46, p_{11} is 0.113, p_{12} is 0.252, which gives a value of 0.22 for ρ_e . For

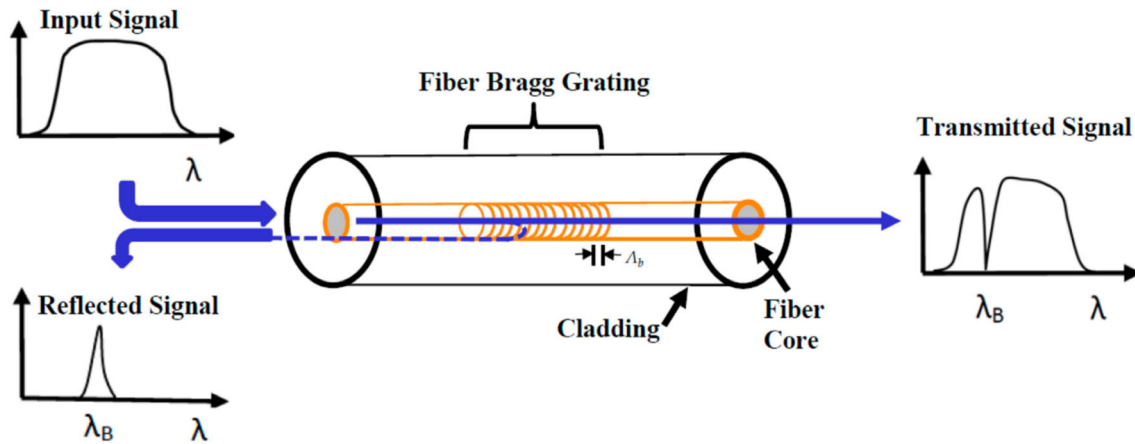


Fig. 1 Principle of fiber Bragg grating (FBG) showing input broadband light signal, reflected signal from the Bragg grating and transmitted signal from the fiber core. Reprinted with permission from Nicolas et al. (2016). <https://creativecommons.org/licenses/by/4.0/>

a grating with a Bragg wavelength of 1550 nm, the strain sensitivity works out to be 1.2 pm/μ ϵ .

The causes for temperature sensitivity of the FBG are thermal expansion i.e., the expansion and contraction of the grating period with temperature, and the thermo-optic effect i.e., change in refractive index with temperature. The Bragg wavelength change with temperature is expressed as

$$\frac{\Delta\lambda_B}{\lambda_B} = (\alpha + \eta)\Delta T \quad (4)$$

where $\alpha = \frac{1}{\lambda} \frac{\partial \lambda}{\partial T}$ is the coefficient of thermal expansion, $\eta = \frac{1}{n_{\text{eff}}} \frac{\partial n_{\text{eff}}}{\partial T}$ is the thermo-optic coefficient and ΔT is the applied temperature. For a silica fiber, the thermal expansion coefficient is $5 \times 10^{-7} \text{ K}^{-1}$ and the thermo-optic coefficient is $7 \times 10^{-6} \text{ K}^{-1}$. The temperature sensitivity evaluates to 11.2 pm/K for a grating with center Bragg wavelength of 1550 nm. The material coefficients α and η are not constant and change with temperature. Equation (4) becomes nonlinear at higher temperatures.

As the light reflected from the Bragg grating is dependent upon the spacing of the index modulation Λ_G and the refractive index n_{eff} , the strain field affects the response of the FBG directly, through the expansion and compression changes of Λ_G and through the strain-optic effect, i.e., the strain-induced change in the glass refractive index. The change in Bragg wavelength $\Delta\lambda_B$ due to an applied strain ϵ_z and temperature drift ΔT is given by

$$\frac{\Delta\lambda_B}{\lambda_B} = (1 - \rho_e)\epsilon_z + (\alpha + \eta)\Delta T \quad (5)$$

where ρ_e is the effective strain optic coefficient, α is the coefficient of thermal expansion of the fiber and η is the thermo-optic coefficient. For a germanosilicate fiber, typical values are $\rho_e = 0.21$, $\alpha = 0.55 \times 10^{-6}$ and $\eta = 8.6 \times 10^{-6}$. Substituting these values in Eq. (1) for an FBG with Bragg wavelength $\lambda_B = 1550 \text{ nm}$, the strain

sensitivity and temperature sensitivity turn out to be 1.22 pm/μ ϵ and 14.18 pm/°C, respectively. Thus, the Bragg wavelength change gives a direct measure of strain and/or temperature. FBG sensors can also be used to transduce other measurands such as pressure, curvature, and vibration into strain. The Bragg wavelength and FBG spectrum is monitored using a broadband FBG interrogator (Mihailov 2012; Othonos and Kalli 1999; Othonos 1997; Hill et al. 1978, 1993; Meltz et al. 1989; Kashyap 1999; Meltz and Morey 1991).

FBG sensors for shock wave measurements

Study of dynamic behavior of materials is essential in various applications like shock and detonation physics, geophysics, particle physics, planetary studies and in several other areas. For predicting dynamic events like high velocity impacts and detonation of explosives, nonlinear wave propagation in solids needs to be understood. Shock compression experiments provide a method to generate such high pressures, high deformation rates to evaluate the material response and provide basis for predicting wave propagation and interaction phenomena. The sudden application of pressure propagates in the material as a discontinuity in density, temperature, stress, enabling the study of Equation of State (EOS), phase diagram, dynamic strength, etc. High pressure loading on the materials under test can be achieved using high velocity impact or explosives. Proper diagnostics must be used in these experiments to measure vital parameters like applied dynamic stress, velocity of the shock wave and shock stress. There are several piezoresistive (carbon, manganin) and piezoelectric (quartz, lithium niobate, PVDF) stress sensors used conventionally (Davison 2008). However, Fiber Optic sensors including FBG sensors owing to their diminutive size

($\sim 200 \mu\text{m}$ diameter of fiber), capability to withstand high pressure shocks, chemical passivity, immunity to electrical sparking and EMI, have been used recently in shock wave diagnostics and detonation experiments (Benterou et al. 2007, 2011; Rodriguez et al. 2013, 2014; Benterou and Udd 2012; Udd and Benterou 2012; Berkovic et al. 2018; Barbarin et al. 2016; Cranch et al. 2013; Udd 2011, 2014; Rodriguez and Gilbertson 2017; Sandberg et al. 2014; Magne et al. 2013).

A fiber optic Fabry Perot Velocity Interferometer system was developed at TNO, Netherlands, to measure speeds of high velocity objects launched by an electric gun. The experimental setup consisted of a laser source, Fabry Perot etalon with lenses, streak camera and optical fiber to transport light between the moving test object and the Fabry Perot interferometer. Doppler shift causes the position of the interferometric pattern formed behind the FP interferometer to change with the object velocity which is recorded by a streak camera. The Fabry Perot system was able to measure velocities in the range of 100 m/s to several km/s (Prinse et al. 2001). Cheng et al., developed a fiber-optic interferometer system consisting of a Sagnac interferometer and Mach–Zehnder interferometer to evaluate the sensitivity of a ‘Composition B’ explosive to high temperature by using a Cook-off tube apparatus. The test explosive was filled in a steel cylindrical Cook-off tube which is heated to several hundred degrees Celsius and its expansion velocity (rate of change of diameter) was monitored by wrapping the sensing fiber arms of Mach–Zehnder and Sagnac Interferometers on the Cook-off tube. The expansion velocity of the tube is an indication of the reaction process of the explosive. The output signals, a measure of change in length of the sensing fibers of the two interferometers, were recorded by a Digital Signal Analyzer (DSA). The expansion velocity of the tube was calculated using fringe counting method and fringe duration methods for MZI and Sagnac interferometers’ output signals, respectively. The results of the fiber-optic interferometers were compared with a thin resistance wire, wrapped on the Cook-off tube at a similar location, and were found to have a better signal-to-noise ratio and detection limit (Cheng et al. 2001).

Van’t Hof et al., first reported the use of FBG sensors for dynamic pressure measurement during detonation of explosives. FBG sensors, owing to their small size do not affect the detonation wave propagation dynamics. Since the building up of pressure in a shock wave exists over a very small area, short length FBG of about 0.5 mm was used to avoid measuring the average pressure over a few mm. The FBG sensor was placed in an ammonium nitrate-based Westfalit D powder explosive in a box with a high-voltage initiator to ignite the explosive (Fig. 2a). The detonation velocity and detonation pressure of the explosive was

2 km/s and 1 GPa, respectively. The wavelength shift of the FBG due to the shock pressure was detected using an unbalanced Mach–Zehnder fiber interferometer with three outputs and three detectors. The Mach–Zehnder interferometer consisted of two FO couplers with two optical paths (Fig. 2b). The three output signals had a fixed phase difference of $2\pi/3$. The wavelength shift was calculated from the phase φ of the interferometric signal. From the shock Hugoniot relation of pressure against specific volume for quartz fiber, the peak detonation pressure was determined. The experimental value of pressure was found to be close to the expected pressure. However, the estimate can be improved as reported, by taking axial compression of fiber along with longitudinal compression (Van’t Hof et al. 2007).

Deng et al. (2011) developed an FBG sensor system to measure shock stress in water using an unbalanced Mach–Zehnder interferometer. A water container with Aluminum target was impacted by an Aluminum flier plate as shown in Fig. 3a with velocity up to 800 m/s, launched from a single stage gas gun to generate stresses up to 1.4 GPa in water. A short length FBG of 2 mm with FWHM of 0.3 nm was used. Based on a linear relation between the refractive index of the FBG and its density (Setchell 1979) under shock loading, a polynomial relation (Barker and Hollenbach 1970) was derived to relate the shock stress in fused silica fiber with the Bragg wavelength shift. The Bragg wavelength shift of the FBG was measured using a fiber Mach–Zehnder interferometer with an optical path difference of 3.1 mm. The unbalanced MZI system consists of a broadband ASE light source (1525–1565 nm) to illuminate the FBG, 2×2 FO coupler to input reflected light from the FBG into the MZI, 3×3 FO coupler at the MZI output which is connected to 3 detectors. The 3 output interferometric signals have a mutual phase difference of 120° . An arctangent data reduction method was used to derive the wavelength shift from the detector signals. The maximum shock stress measured by the sensor was 1.4 GPa with an accuracy of 10% (Fig. 3b).

Ravid et al. (2014) studied the response of FBGs to weak planar shock wave with shock pressure under 1 GPa. The dependence of orientation of FBG with the incoming shock front and the effects of photoelasticity and dynamic strain on the FBG were estimated theoretically. When the shock front travels parallel to the FBG axis, the fiber gets compressed reducing the grating period Λ along with change in effective refractive index n_{eff} of FBG due to material density changes (photoelastic effect) which results in Bragg wavelength shift of -14 pm/MPa . When the shock front travels perpendicular to the FBG axis i.e., the planar shock wave strikes the fiber from the side, only the photoelastic effect is predominant. This causes a Bragg shift of 9 pm/MPa . In the test setup as shown in Fig. 4a,

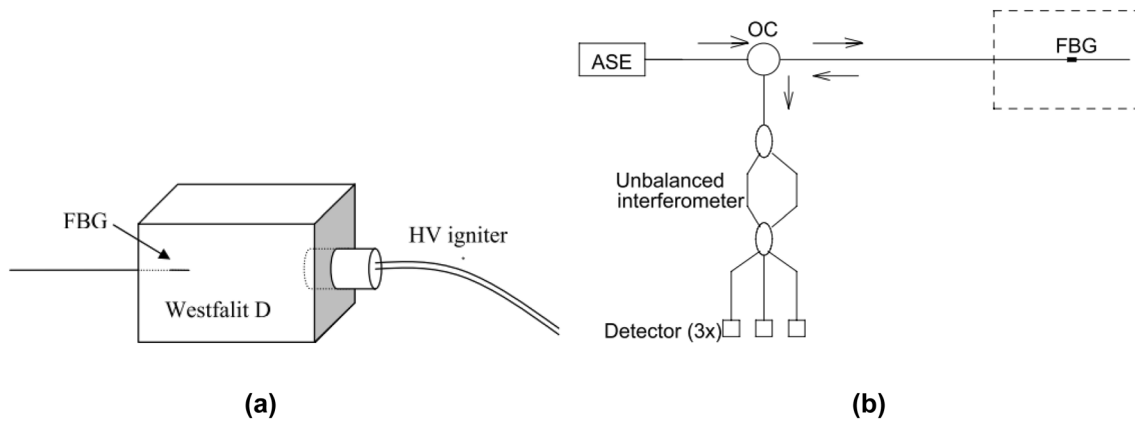
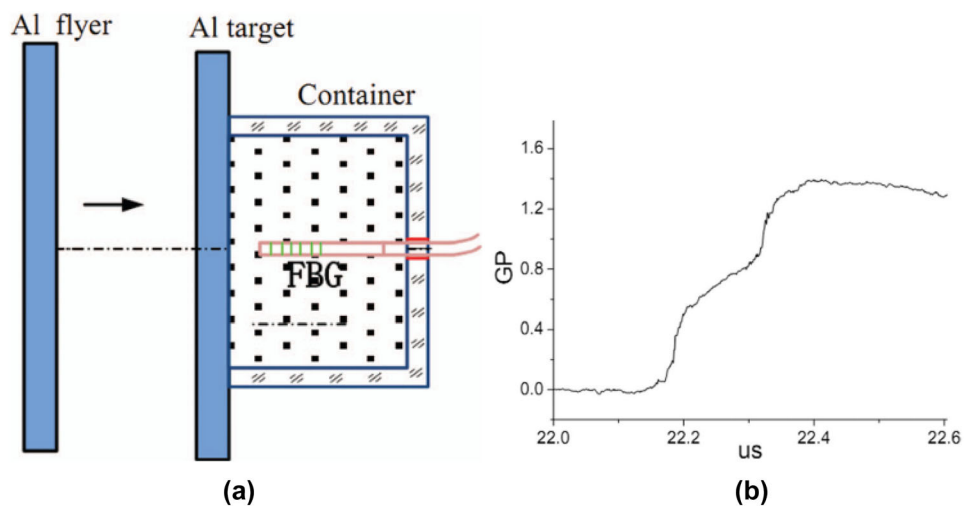


Fig. 2 **a** Schematic of test setup with FBG, explosive and HV igniter, **b** schematic of the unbalanced Mach–Zehnder interferometer. Reprinted with permission from Van't Hof et al. (2007). Copyright 2007, Society of Photo-Optical Instrumentation Engineers (SPIE)

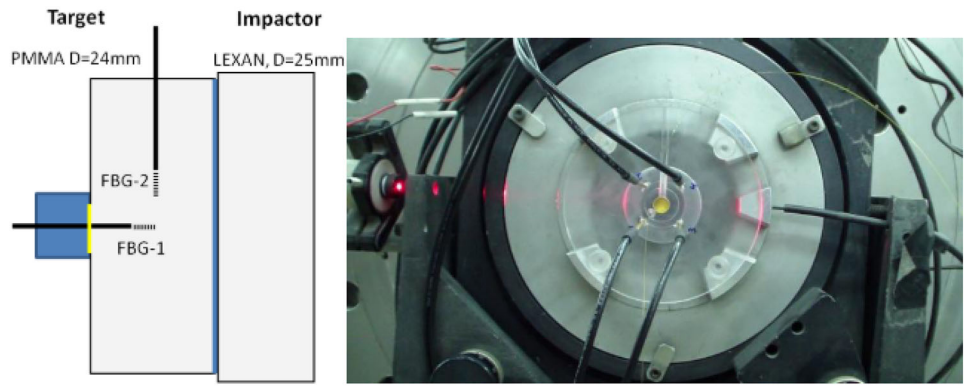
Fig. 3 **a** Schematic of the test setup for measuring shock stress in water, **b** shock stress in water. Reprinted with permission from Deng et al. (2011). Copyright 2011, American Institute of Physics



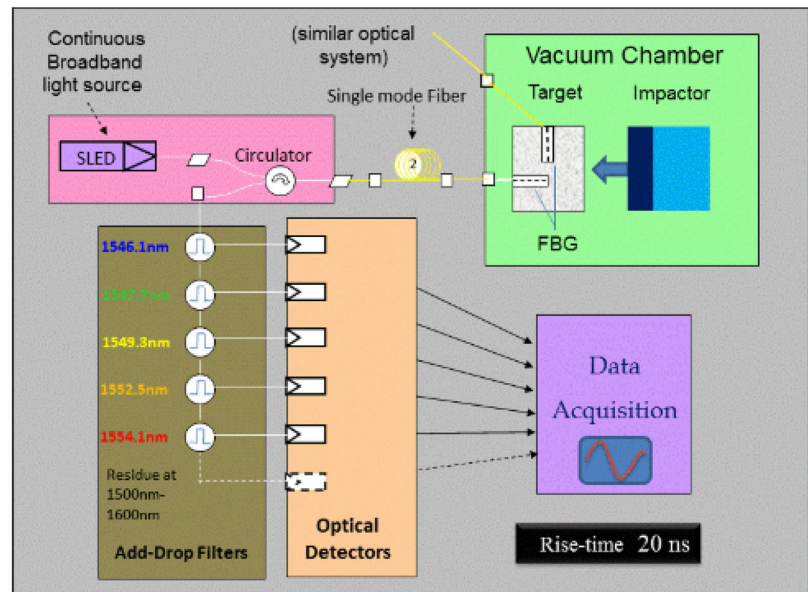
two short length FBGs ($L = 1$ mm, $\lambda_B = 1552.5$ nm) were embedded in a PMMA target, with one parallel and the other perpendicular to the incoming shock front. Short length FBGs are used to match with the dimension of shock wave region and measure the pressure at a point instead of average pressure. The target was struck with a high velocity (300 m/s) LEXAN impactor launched from a gas gun. VISAR was used to measure the particle velocity by using a gold-coated PMMA window. The authors used an electro-optical readout system consisting of add-drop filters with different spectral windows, which were then connected to high speed detectors (Fig. 4b). This is described in detail in Ravid et al. (2014). The experiments showed that FBG survived for more than $1 \mu\text{s}$ under 5 kbar shock stress. The stresses measured were approximately 4.6 kbar for shock front traveling parallel to FBG axis and 1.8 kbar for the other case. However, the accuracy of the results could be improved.

The major challenges in monitoring shock waves with FBGs are (a) understanding the ultra-fast changes caused by shock waves on the material and spectra of FBG (b) development of interrogation techniques to acquire the spectral changes at the rate of GHz. Shafir et al. (2017) extended the work on shock wave measurements with FBGs. Stainless steel impactor at projectile velocity of 315 m/s was used to generate planar shock wave of magnitude 0.58 GPa in a water chamber. Two short length FBGs ($L = 1$ mm), one perpendicular and one parallel to the direction of propagation of shock front, were used to measure the shock strength in water (Fig. 5a). A broadband SLED source was used to illuminate the FBG and the FBG reflected signal was directed to 6 DWDM add-drop filters with 1.2 nm bandwidth with each channel having a wavelength separation of 1.6 nm. The output of each channel was connected to fast InGaAs photodetectors (Fig. 5b). For the FBG with axis parallel to the direction of shock propagation, the compressive strain effect (reduction

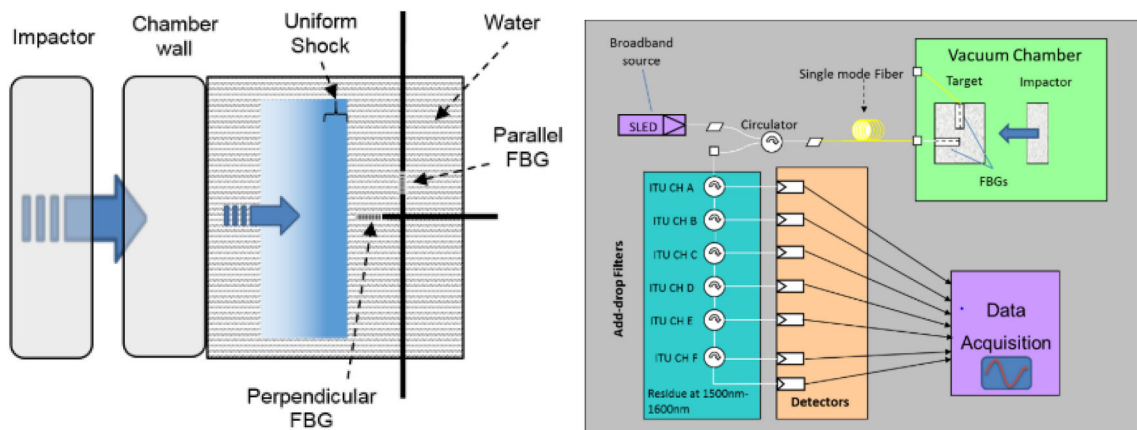
Fig. 4 **a** Schematic and photograph of PMMA target setup, **b** electro-optical readout system. Reprinted with permission from Ravid et al. (2014). <https://creativecommons.org/licenses/by/3.0/>



(a)



(b)



(a)

(b)

Fig. 5 **a** Schematic of the experimental setup, **b** optical measurement setup. Reprinted with permission from Shafir et al. (2017)

in λ) dominates the photoelastic effect. The wavelength shift was -3.2 nm for shock strength of 5.8 kbar, giving a shock pressure sensitivity of -5.5 pm/MPa. Similarly, for an FBG with axis perpendicular to the shock propagation direction, the photoelastic effect dominates. The wavelength shift was 5.5 nm for shock amplitude of 5.8 kbar, resulting in a pressure sensitivity of 9.5 pm/MPa.

Hsu et al. (2020) used FBG sensors to measure the strain of underwater structure subjected to shock loading from underwater explosion. The experimental setup consisted of a thin cylindrical shell ($t = 1$ mm) made of 5086 aluminum alloy of diameter 500 mm in a static water tank (Fig. 6). FBG sensor was bonded on the inner surface of the cylindrical shell in axial direction to measure the strain on the cylinder surface caused by the impact of shock wave. Shock waves were generated by explosion of 1 g TNT explosive at fixed depths of 30 cm, 15 cm, 5 cm below the cylindrical shell. FBG sensor was calibrated initially using a four-point bending test and was found to have a strain sensitivity of 1.4 pm/ $\mu\epsilon$. The FBG signals were acquired using a spectrometer arrangement. The explosion test time was 0.5 to 1 s. The FBG wavelength shifts were found to be 2.563 nm (30 cm depth), 37.135 nm (15 cm depth) and 32.923 nm (5 cm depth). As the tests were done continuously which might have caused the plastic deformation or yielding of the cylindrical structure (shock stress greater than yield stress of aluminum), the wavelength shift at 5 cm depth was found to be inconsistent with the other readings. However, FBG sensor with its high sensitivity, stability, and repeatability can be used in these extreme environments to measure shock induced strain with improved design of the test structure.

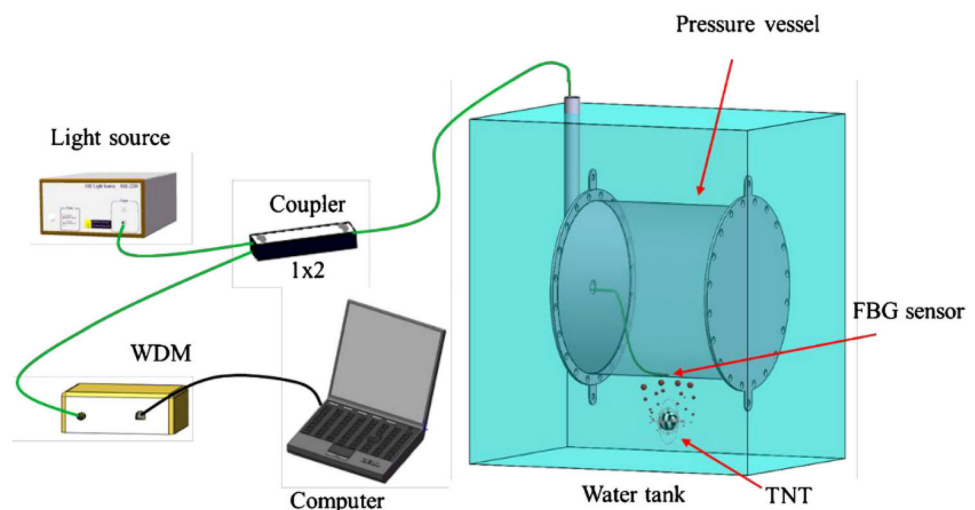
FBG sensors for ground-based aerodynamic test facilities

FBG sensors for monitoring evacuation process

Vacuum environment is necessary for several industrial and scientific research like microelectronic industries, nanoscale device fabrication processes, metallurgical processes, aerodynamic test facilities like wind tunnels, shock tunnels and many others. The level of vacuum in an enclosed volume is determined by measuring the absolute pressure inside. Pirani and Penning gauges have been used for vacuum measurement for a long time since their invention. Pirani gauges are used in the pressure range of 10^{-3} to 10 mbar and Penning gauges are used from 10^{-2} to 10^{-7} mbar (Jitschin and Ludwig 2004). Pirani gauges work on the principle of thermal conductivity changes of a heated metal wire as a function of pressure which is measured using a Wheatstone Bridge configuration. But they are bulky, require regular calibration and heating time of metal wire is high. Miniaturized vacuum sensors based on MEMS technology have lower fabrication cost, lower power consumption, improved dynamic range but its implementation in vacuum environments is complex requiring several electrical connections, feedthroughs, and metal flanges. Also, electrical-based sensors suffer from EMI. Hence FBG sensors offer a viable alternative for vacuum measurement.

Guru Prasad et al. (2010) demonstrated the use of FBG sensors for real-time monitoring of evacuation process and leak detection in a bell jar vacuum chamber. The measurement principle was based on the pressure induced Bragg wavelength shift of FBG sensor. The vacuum chamber capable of creating a vacuum of 0.1 millibar was fitted with a Pirani gauge to validate the FBG measurements simultaneously. The Bragg wavelength was

Fig. 6 Experimental setup of FBG underwater shock test. Reprinted with permission from Hsu et al. (2020). Copyright 2020, Elsevier



monitored using SM 130 Micron Optics interrogator at an acquisition rate of 1 kHz. An optical fiber vacuum feed-through (OFVFT) was designed to interface the fiber to the vacuum chamber with the FBG positioned inside the chamber. Pressure inside the bell jar was reduced from atmospheric pressure to 1 mbar and evacuation process was monitored using FBG sensor and Pirani gauge. The FBG sensor showed a linear response during evacuation process, closely following the Pirani gauge response. When the vacuum was held constant, the FBG center wavelength showed a slight increase instead of a flatline response which required further investigation (Fig. 7a). During evacuation, the Bragg wavelength decreases due to compression of the FBG. The FBG sensor showed a Bragg wavelength shift of 45 pm for a vacuum pressure change of 80 mbar reading on Pirani gauge. The experimentally obtained pressure sensitivity of FBG sensors was 5.625 nm/MPa compared to a theoretical pressure sensitivity of 5.6 nm/MPa. The FBG sensor was used in a pressure range of 1 bar to 1 mbar. The FBG sensor response was also recorded during the entire process of evacuation, constant vacuum, and vacuum release (Fig. 7b).

FBG sensors for hypersonic wind tunnel measurements

Surface measurement of pressure and temperature during aircraft testing is essential for the optimization of structural design, choice of materials and life estimation. Modern space missions, missile programs, supersonic flight programs require research and analysis of complex high-speed flow fields in hypersonic and supersonic regimes. These

high-speed flow fields are characterized by high temperature, pressure, flow enthalpies. To simulate these flow conditions on ground, impulse test facilities like wind tunnels, shock tubes are used. These ground-based test facilities are limited by short test times owing to the need to withstand high thermal and structural loads. Typical test times in shock tunnels are in the order of milliseconds. The harsh flow conditions, sudden variations accompanied with short test times impose challenges in implementation of flow diagnostics in these test facilities. Estimation of crucial parameters like aerodynamic forces and moments on aircraft structures, drag in high-speed flows and flow unsteadiness requires surface pressure measurements (Aime et al. 2019; Chehura et al. 2009; Lawson et al. 2016; Segawa et al. 2003; Jukes et al. 2012; Yu et al. 2022). Surface temperature measurements are important for determination of thermal loads on the aircraft structure. Because of the short run times and extreme flow conditions in shock tunnels, the pressure sensors should have fast response time and withstanding capabilities. High temporal and spatial resolution of sensors is important in certain flow measurements. For pressure sensing, electrical-based sensors like fast response piezoelectric PCB and piezoresistive Kulite sensors, pressure sensitive paints (PSPs) for surface pressure distribution in high-speed wind tunnels, pin-hole static pressure probes, micro-electro mechanical systems (MEMS)-based pressure sensors have been used (Sriram et al. 2015). Conventionally used temperature sensing devices for hypersonic flow fields and test models include thermocouples, resistive temperature devices (RTDs) and infrared cameras. But some of the electrical-based sensors suffer from cumbersome connections, complex lead wire extensions and adapters, expensive high precision data

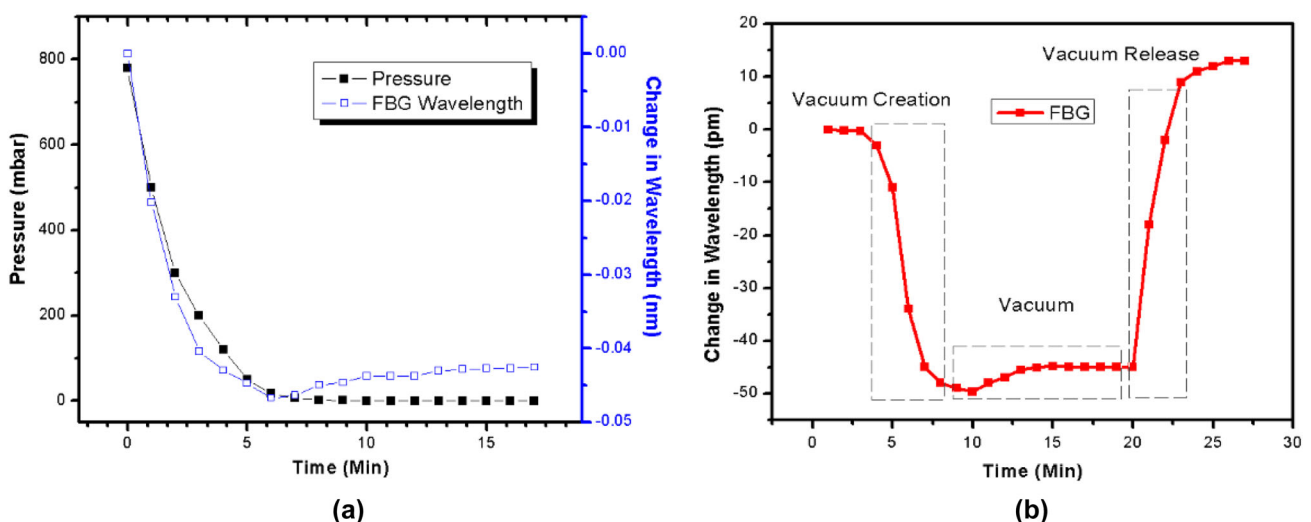


Fig. 7 **a** Comparison of FBG and Pirani gauge response during evacuation, **b** FBG response during evacuation and vacuum release. Reprinted with permission from Guru Prasad et al. (2010). Copyright 2010, Society of Photo-Optical Instrumentation Engineers (SPIE)

acquisition systems and electronics, noise pickup and EMI. FBG sensors with their small size, multiplexing capability and fast response can give high spatial and temporal resolution measurements in ground-based aerodynamic test facilities (Qiu et al. 2020).

Guru Prasad et al. (2013) demonstrated the use of FBG sensors for measurement of pressure and temperature on 30° apex angle blunt cone test specimen in hypersonic wind tunnel at IISc, Bengaluru. The FBG temperature sensing probe was designed by encasing the FBG sensor in a 200 µm stainless steel tube to isolate strain effects but conduct heat into the FBG. The steel tube encapsulated FBG temperature probe was calibrated and found to have a temperature sensitivity of 10 pm/K, similar to a bare FBG sensor. The carbon fiber blunt cone specimen was placed in the 300 mm diameter test section of the hypersonic wind tunnel facility which is described in Kishore et al. (2005). The angle of attack of air flow on the specimen was 0°. Two 3 mm gauge length FBG sensors were used. One bare FBG, sensitive to both pressure and temperature (Pressure FBG) and FBG temperature sensor probe were surface bonded on the leeward side of the specimen. Temperature compensation was done by subtracting the Bragg shift of temperature probe from the Pressure FBG. Bragg wavelength from both the sensors was acquired simultaneously using Micron Optics SM130 interrogator at a sampling frequency of 1 kHz. The experiments were carried out at hypersonic flow speeds of Mach 6.5 and 8.35. The FBG temperature sensor recorded 326 K at Mach 6.5 and 334 K for Mach 8.35 with the ambient temperature of 298 K (Fig. 8a). FBG pressure sensitivity of 464.12 pm/bar was used to calculate pressure from Bragg wavelength shift (Correia et al. 2007). The gauge pressure measured by the FBG sensors was 0.05 bar for Mach 6.5 and 0.07 bar for Mach 8.35 (Fig. 8b). The temperature and pressure measurements were validated with CFD simulations and were found to be in good agreement.

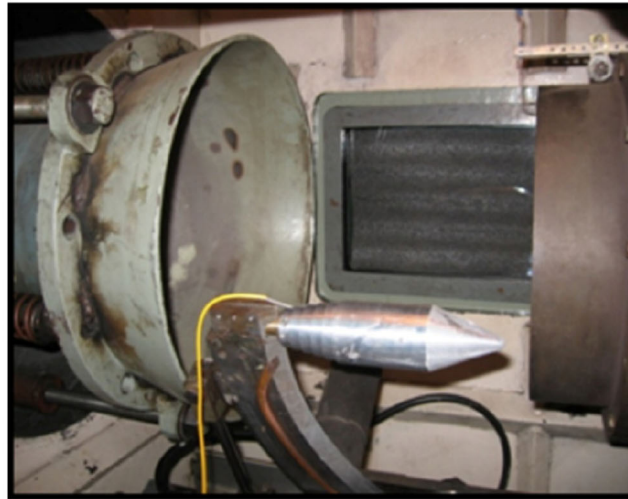
FBG sensors for structural health monitoring

Real-time in situ monitoring of aircraft composite structures is necessary for assessment of their performance and integrity. Several types of sensors like strain gauges, ultrasonic sensors, passive acoustic sensors, etc., have been explored for SHM applications. But some of these sensors are difficult to deploy over large structures, incapable of withstanding harsh environments and low operational lifetime. Fiber optic sensors, especially Fiber Bragg Grating (FBG) sensors have proved to be excellent candidates due to their numerous advantages such as small size, lightweight, durability, chemical passivity, immunity to electromagnetic interference, serial multiplexability and

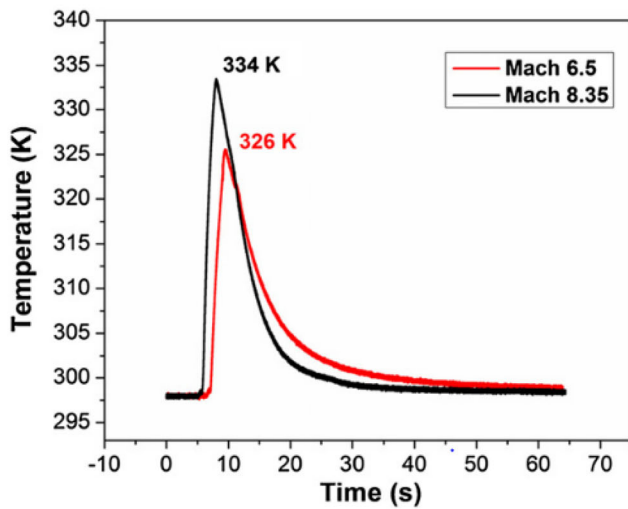
possibility of embedding the sensor within the structure. Today, structures of civil aircrafts and military airplanes are composed of a high percentage of advanced composite materials. This is due to their low weight-to-strength ratio compared to conventional metallic materials thereby improving fuel efficiency, operational costs, reducing emissions and lowering manufacturing/certification costs of future aircrafts.

However, composite materials are anisotropic being composed of different materials (matrix and fibers) which makes them more complex than their metallic counterparts. Durability and safety issues arise like initiation and propagation of failure cracks caused by impact loads and the estimation of remaining strength and residual life of the structure. Intelligent monitoring systems that would enable continuous in-service load monitoring and damage detection of aircraft structures are essential. The added advantage of integrating FBG sensors into composite materials during the layup process would also enable the monitoring of composite structures during their whole life cycle, improving their safety, reliability, cost efficiency and, hence extending their operational life. FBG-based sensors and measurement systems are already being employed in load and damage monitoring of aircraft composite structures, mainly in ground tests and design. However, its widespread usage is still impeded by problems like sensor performance when embedded, detection capability, maintainability, size, and weight of the interrogation equipment (Di Sante 2015; Hegde and Asundi 2003, 2006; Lee et al. 2003; Floris et al. 2021; Jinachandran and Rajan 2021; Rocha et al. 2021; Kuznetsov et al. 2021; Kahandawa et al. 2012).

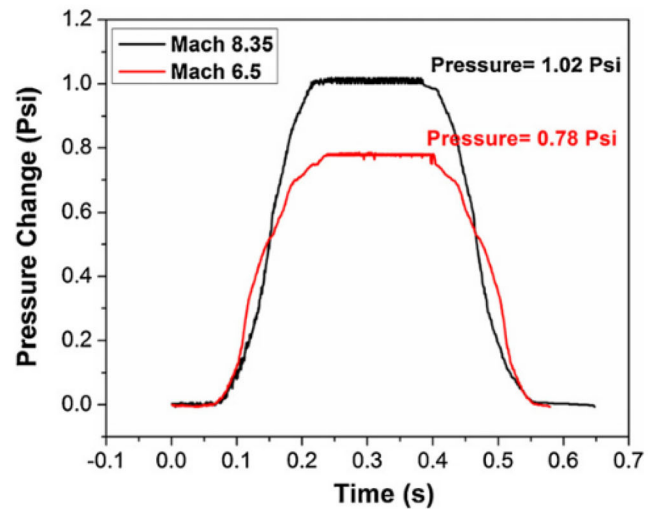
Goossens et al. (2021) demonstrated the use of surface mounted FBG sensors for the detection of barely visible impact damage (BVID) on aerospace grade carbon fiber-reinforced plastic (CFRP) laminates. The detection principle was based on the change in optical signal before and after impact. A BVID causes change in strain field around the area of impact location which results in non-uniform strain acting on the FBG nearby (Fig. 9a, b). Bragg wavelength shift (measure of magnitude of strain change) and Pearson correlation coefficient (Comparison of FBG spectrum before and after impact) were used as damage indicators. Ormocer-coated Draw Tower Gratings (DTG) with FBG length of 8 mm were used. Each fiber had 6 wavelength multiplexed FBGs with an inter-FBG separation of 26 mm. The BVID detection thresholds of FBG sensors in the presence of standardized on-ground aircraft conditions, namely temperature (− 45 to 50 °C) and vibration levels, was investigated with four CFRP material systems (thermoset, a dry fiber and liquid resin, thermoplastic, CNT-infused thermoset). With Bragg wavelength shift damage indicator, BVID could be detected up to a



(a)



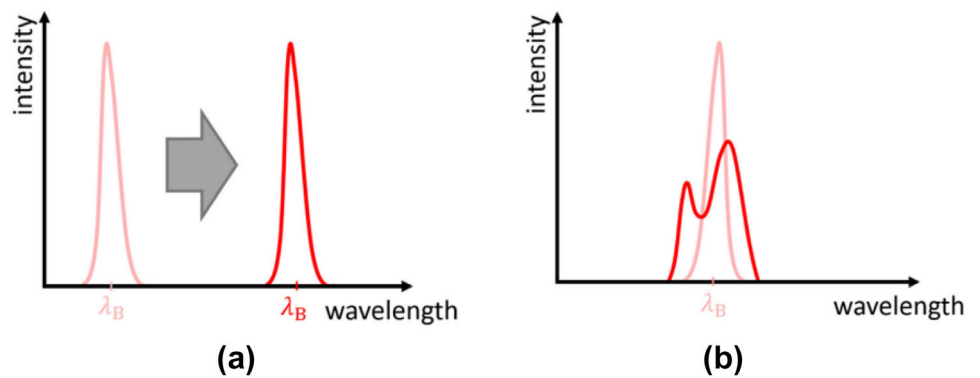
(b)



(c)

Fig. 8 **a** Photograph of the blunt cone specimen in hypersonic wind tunnel, **b** time response of FBG temperature sensor, **c** time response of FBG pressure sensor. Reprinted with permission from Guru Prasad et al. (2013). Copyright 2013, IOP Publishing Ltd

Fig. 9 **a** Bragg wavelength shift caused due to uniform strain, **b** FBG peak distortion due to non-uniform strain. Reprinted with permission from Goossens et al. (2021)



(a)

(b)

distance of 17–35 mm from fiber array for different CFRP material systems. For BVID with delamination of CFRP reaching below the FBG array, Pearson correlation coefficient (a measure of peak distortion) could detect BVID up to a distance of 12.3 mm from FBG array.

FBG sensors in space applications

Continuous monitoring of spacecraft during its fabrication, testing and service is important for its successful operation in space mission. Fiber optic sensors offer several advantages over the conventional electrical sensors due to their lightweight, immunity to EMI and electric sparking, flexibility of fiber optic cable for ease of embedment in complex structures, multiplexability of several sensors, chemical passivity which allows deployment in hazardous environments, high sensitivity, and remote interrogation. All these features make fiber optic sensors suitable for harsh conditions in space viz., space radiation (gamma rays, heavy ions), microgravity, thermal fluctuations, outgassing due to vacuum, vibrations, and shock (Mckenzie and Karafolas 2005). Several space agencies like NASA and ESA have developed, designed, tested and implemented fiber optic sensors including FBG sensors in various spacecraft components to measure a multitude of parameters. Some of the major applications of fiber Bragg gratings are in.

High pressure measurement in space applications using diaphragm-based FBG sensor

High accuracy pressure measurement is necessary in various space subsystems like propulsion, structure and payload monitoring (Mckenzie and Karafolas 2005). Harsh conditions in space such as large thermal fluctuations, gamma radiations, heavy ions, microgravity, shock and mechanical vibrations make fiber optic sensing systems which are immune to Electromagnetic interference (EMI), electrical sparking and explosive environments, excellent candidates for sensing applications in space. Fiber Bragg Grating (FBG) sensors owing to their wavelength-encoded output and serial multiplexability have been explored in various space applications for measuring strain, temperature, pressure, etc. Hegde et al., developed a diaphragm-based FBG sensor with temperature compensation for high pressure measurement (up to 700 bar gauge) with over-range capacity of 1.5 times the maximum operating pressure (1050 bar) and burst pressure of twice the maximum operating pressure (1400 bar). The operating media was cryogenic propellants for rockets, missiles and launch vehicle applications (Hegde et al. 2021).

The pressure sensor was composed of a compact diaphragm (radius 12.5 mm and 2.02 mm thickness) and pressure port assembly made of martensitic stainless steel (APX-4) owing to their excellent mechanical properties even at elevated temperatures. Polyimide-coated FBG was bonded on the diaphragm center for pressure measurement and a temperature compensating FBG was bonded on the sensor body in a strain-free region (Fig. 10a). The sensor assembly was mounted on a hydraulic dead weight tester and calibrated up to the maximum pressure of 700 bar. The Bragg wavelength data was acquired using a SmartFibers FBG interrogator with a wavelength stability of 5 pm. The sensor showed a good pressure sensitivity of 3.64 pm/bar and a nonlinearity + Hysteresis error of 0.75% of full-scale pressure in the range of 0 to 700 bar, with a correlative coefficient of 99.99% (Fig. 10b). The minimum pressure or the threshold of the sensor was found to be 0.4 bar (0.057% of full scale). These were found to exceed the requirements for the specific application. A strain transfer analysis was carried out using Comsol Multiphysics to verify the strain transfer efficiency between the diaphragm surface to the FBG as well as optimize the polyimide coating thickness of the FBG sensor. The pressure sensor was compensated for temperature fluctuations in the full operating range of -40 to 90 °C required in space environment and recalibrated for pressure in the hydraulic dead weight tester. The error was found to be within the tolerance limit for the application and depend upon the operating temperature range of the adhesive.

The impulse/dynamic response of the pressure sensor was tested in a table-top manually driven, diaphragm-type shock tube called “Reddy tube.” The pressure sensor was mounted on the end flange/open-end of the shock tube (Fig. 11a). The Bragg wavelength was recorded at a sampling rate of 2.5 kHz using SmartFibers FBG interrogator. The driver gas was nitrogen and the driven tube was open at the atmospheric pressure. The shock pressure test was carried out at driver pressures of 18.5 bar and 19.9 bar at Mach numbers of 4.59 and 5.5, respectively. The peak Bragg wavelength shift was 68 pm for driver pressure of 18.5 bar (Fig. 11b). The sensor was recalibrated and tested for its performance after shock test in the same pressure range of 700 bar and it was found to be within an error of 1% of full scale (700 bar).

Vibration tests were carried out by mounting the pressure sensor on an electrodynamic shaker connected to a vibration controller (M/s Sdyn) to simulate the vibrations encountered by the aerospace systems and sub-assemblies during their operation. The vibration and acoustic load experienced by launch vehicle components and its sub-systems during lift-off and atmospheric re-entry can be detrimental to the structural integrity of the aircraft. The experiments were carried out at LPSC Bengaluru. Two

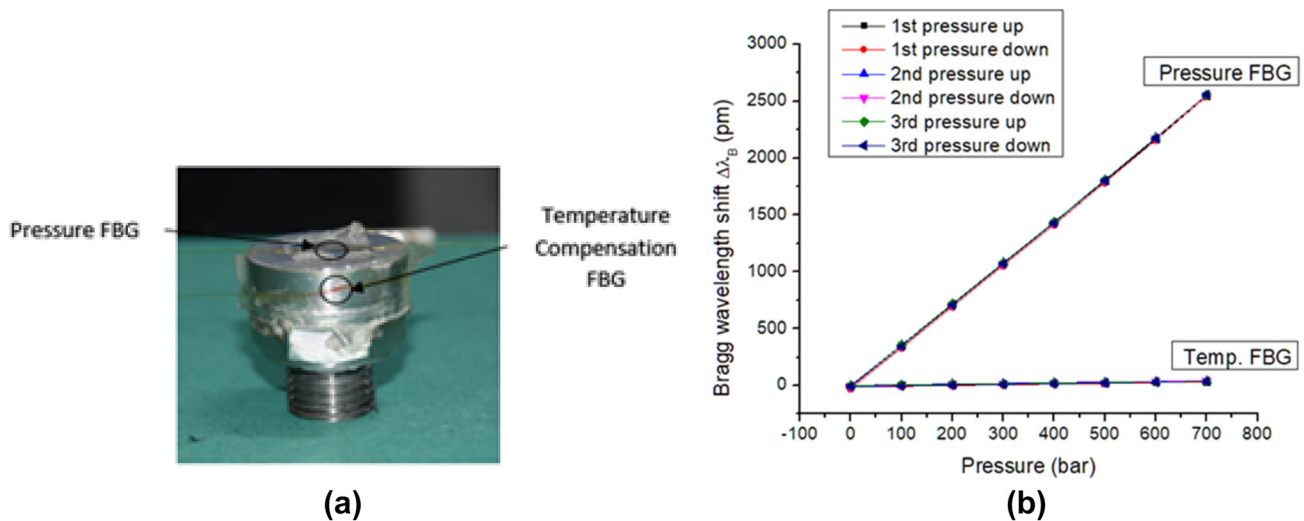


Fig. 10 **a** FBG pressure sensor with location of bonded pressure and temperature compensation FBGs. **b** Calibration plot of FBG pressure sensor along with temperature compensation sensor. Reprinted with permission from Hegde et al. (2021)

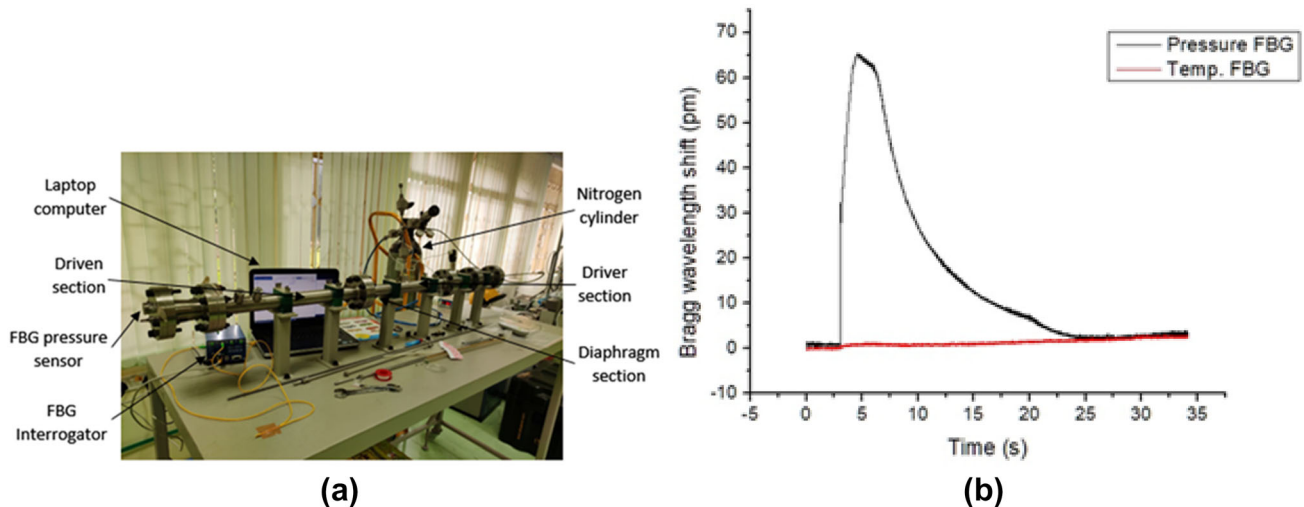


Fig. 11 **a** Photograph of the FBG pressure sensor mounted on the shock tube and connected to FBG interrogator, **b** time response of pressure sensor to passing shock wave with 18.5 bar driver pressure. Reprinted with permission from Hegde et al. (2021)

kinds of vibration tests were carried out based on standard vibration levels for flight acceptance and qualification initially determined by acoustic testing on flight sub-assembly. The vibration tests were carried out to determine the response of the FBG pressure sensor to vibrations and evaluate the robustness, durability and identify any damages caused by vibration. Swept sine vibration test was carried out using a sine controller that produced a swept sine signal. The test was carried out in both longitudinal and lateral axes of the sensor at specified acceleration (g) and displacement (mm) levels. A displacement level of 15 mm was used from 10–16 Hz and acceleration of 10 g from 16–100 Hz for vibration test along longitudinal z -

axis. The frequency sweep rate was 2 octaves per minute. Random vibration test was carried out with all frequencies present simultaneously without any periodicity. The acceleration level used was 13.5 g rms with a test duration of 120 s. In sine vibration test, the maximum error induced by vibration along longitudinal z -axis for pressure measurement was 1.2 bar which was 0.17% of full scale pressure (700 bar). In random vibration test, the maximum pressure measurement error in presence of vibration along longitudinal axis was 1.5 bar (0.21% of full scale pressure) (Fig. 12a). The FFT of FBG response to random vibrations revealed that the FBG sensors were found to be almost insensitive to high frequency vibrations (Fig. 12b).

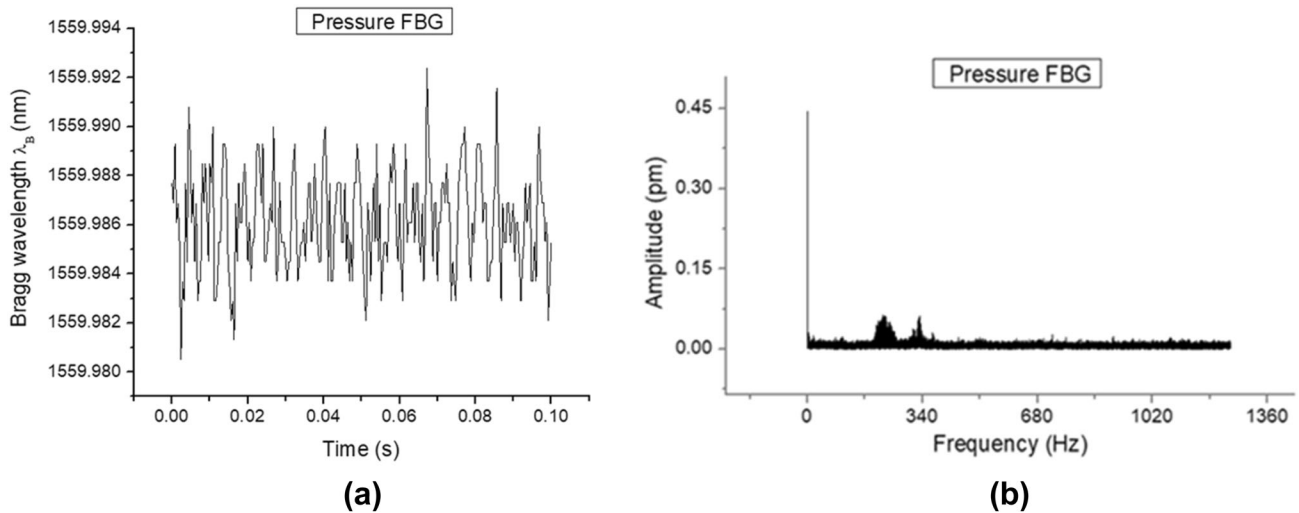


Fig. 12 **a** Plot of random vibration test, **b** FFT plot of random vibration response. Reprinted with permission from Hegde et al. (2021)

Spacecraft/satellite structural health monitoring

Satellites with their sophisticated structure, and electrical connections require continuous monitoring of thermal and structural design for ensuring their reliability throughout their lifecycle. During manufacturing, its necessary to monitor micro cracks or damages and thermal stresses if any to ensure efficient fabrication process. Satellites are subjected to harsh environment tests like thermal vacuum test, vibration test, acoustic emission test and static load test to simulate the space environment. Conventional sensors like thermocouples (temperature), strain gauges (strain), accelerometers (acceleration), acoustic emission sensors must be installed and detached after each test. For such tests, FBG sensor network can be implanted in composite structures to monitor a variety of parameters with higher sensitivity, lower costs, and enable shorter lead times. Even during its operation in orbit, the FBG network can provide continuous information about impact from debris and thermal stresses. Kabashima et al., developed a health monitoring system using FBG sensors in satellite structure. They developed an FBG sensor network which was embedded in the composite laminate structure of satellite. The sensor network was used to detect damage, thermal stresses induced during curing and gluing phases of the fabrication process (Smart manufacturing). An optical fiber connector compatible with different cladding diameter fibers was developed that could be embedded in composite laminates. Strain and temperature measurements on an embedded heat-pipe composite panel, a satellite structure, were carried out using 2 FBG sensors (temperature and strain) in a vacuum thermal chamber and results compared with thermocouple readings and FEM analysis.

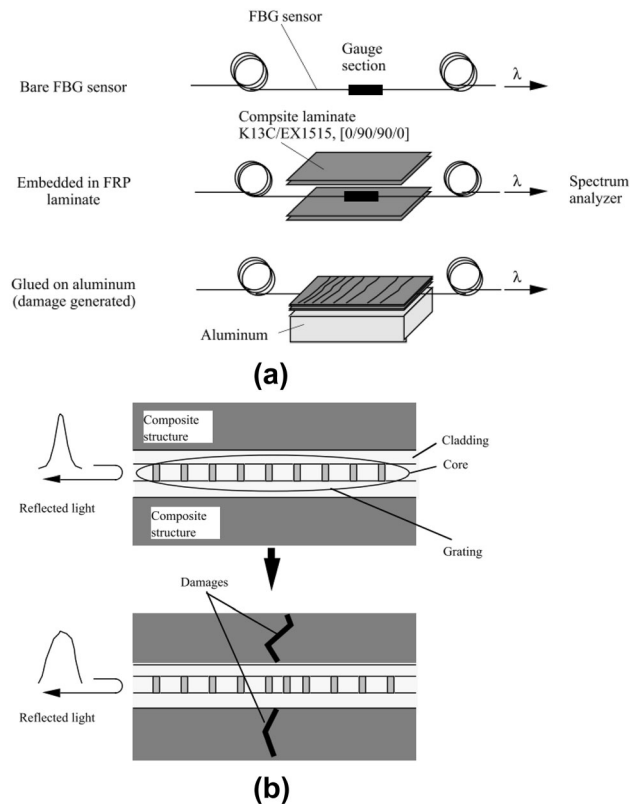


Fig. 13 **a** Change in FBG spectral shape due to non-uniform strain caused by damage, **b** FBG sensor network embedded in composite for damage detection. Reprinted with permission from Kabashima et al. (2001). Copyright 2001, Society of Photo-Optical Instrumentation Engineers (SPIE)

Damage detection in composite laminates due to thermal stresses was carried out by embedding FBG sensors in composite laminates and analyzing spectral shapes of

reflected light. It was found that the FBG spectral shape changed due to non-uniform strain caused by damages on the composite plate (Fig. 13) (Kabashima et al. 2001).

Ecke et al., developed a structural health monitoring system using a network of 12 FBG sensors for measurement of strain and temperature on a crew return vehicle prototype, X-38 for the ISS. To maintain the system stability in challenging space environment (high vacuum, random vibration of 10 g rms, 20 g shock acceleration), the fiber was coated with organic modified ceramic (Ormocer) and passivated with silane compounds for protection against humidity and corrosion. The temperature measurement range was -40 to 200 °C and -1000 to 3000 $\mu\epsilon$ for strain during the lifecycle (launch, orbit, and re-entry) of the spacecraft. A robust data acquisition unit was developed consisting of a superluminescent diode (SLD) source and polychromator. A good repeatability of 25 $\mu\epsilon$ for strain and 1 °C for temperature was obtained (Ecke et al. 2001).

Reusable Launch Vehicles need a more advanced Structural health monitoring system compared to the expendable launchers without affecting the mission and affordable at a reasonable cost (Renson 2003). Diaz et al., developed a Structural Health monitoring system by embedding FBG sensors in the CFRP fuselage of Reusable Launch Vehicle (RLV) for a technology development programme of the ESA (Diaz et al. 2003).

FBG sensors for monitoring of cryogenic spacecraft tank structures

Latka et al., developed an FBG-based temperature, strain, and hydrogen monitoring sensor system for cryogenic liquid hydrogen tanks for the ESA. For the detection of hydrogen leakage, a pair of fiber Bragg gratings (FBG) inscribed in a hydrogen loaded D-shaped elliptical core high-birefringent fiber is used with the grating at the fiber end glued to a palladium foil. The palladium foil deforms when it absorbs hydrogen causing a corresponding Bragg shift. Temperature compensation was accomplished by bonding a second FBG close to the hydrogen sensor. Strain sensor head consisted of 2 polyimide and Ormocer-coated FBG sensors bonded orthogonally for 2-D strain measurements in the range of -1000 to 3000 $\mu\epsilon$ in the inner wall of hydrogen tank. Temperature measurement in the range of 20 to 300 K was carried out with an FBG sensor encapsulated in a protective tube for strain isolation. The data acquisition unit consisted of a broadband light source and data processing unit (Latka et al. 2004).

Dynamic strain monitoring of antenna reflector during acoustic qualification tests

Friebele et al., demonstrated the use of FBG sensors for measurement of dynamic strain in lightweight antenna reflector in spacecraft during acoustic qualification tests. The effects of embedding optical fibers on the strength reduction in composites, issues of fiber leads, fiber ingress-egress were studied. The parabolic reflector, with a graphite membrane reflector surface, was fabricated from graphite-epoxy elements with metal epoxy fittings. Two arrays of four FBGs were attached on various points of the reflector structure such as struts, membrane and support rings as shown in Fig. 14a. Resistance strain gauges were also used for verification of FBG measurements. The Bragg wavelength was monitored using unbalanced Mach-Zehnder interferometer and digital audio tape recorder with an acquisition rate of 5 – 2000 Hz. The FBG signals were found to be in good agreement with RSG signals having a low noise apparent strain of < 1 $\mu\epsilon$ (Fig. 14b) (Friebele et al. 1999, 2004).

Measurement of pressure and temperature in propulsion subsystem

Propulsion subsystem produces thrust for controlling and maneuvering the spacecraft in space. A variety of sensors are used for monitoring several important parameters which are crucial for mission operation. PROBA (Project On-Board Autonomy) are small low earth orbit satellites of the ESA for demonstrating and testing new spaceflight technologies. The hybrid cold gas—solid gas generator propulsion subsystem of the PROBA II consisting of a Xe tank, solid gas generator, plenum and thruster, requires monitoring of pressure (0 – 45 bar) and temperature (-40 to 400 °C on thrusters, -40 to 70 °C on fuel tanks and connecting fuel pipes) for ensuring performance and operational safety (Fig. 15). Serially distributed wavelength multiplexed FBG sensors on several fiber optic lines constituting a fiber optic harness are connected to a single central interrogation unit on-board PROBA II. The FBG pressure sensor had better resolution and dynamic characteristics (2 mbar, 10 Hz) than existing electrical sensors. The FBG temperature sensor had resolution of 0.1 °C. The multiplexability of several sensors reduces the weight of the overall fiber optic demonstrator (FSD) system (Mckenzie and Karafolas 2005).

Thermal control in satellite structure panels

Temperature measurement is required in a satellite's communication module (CM) and service module (SM).

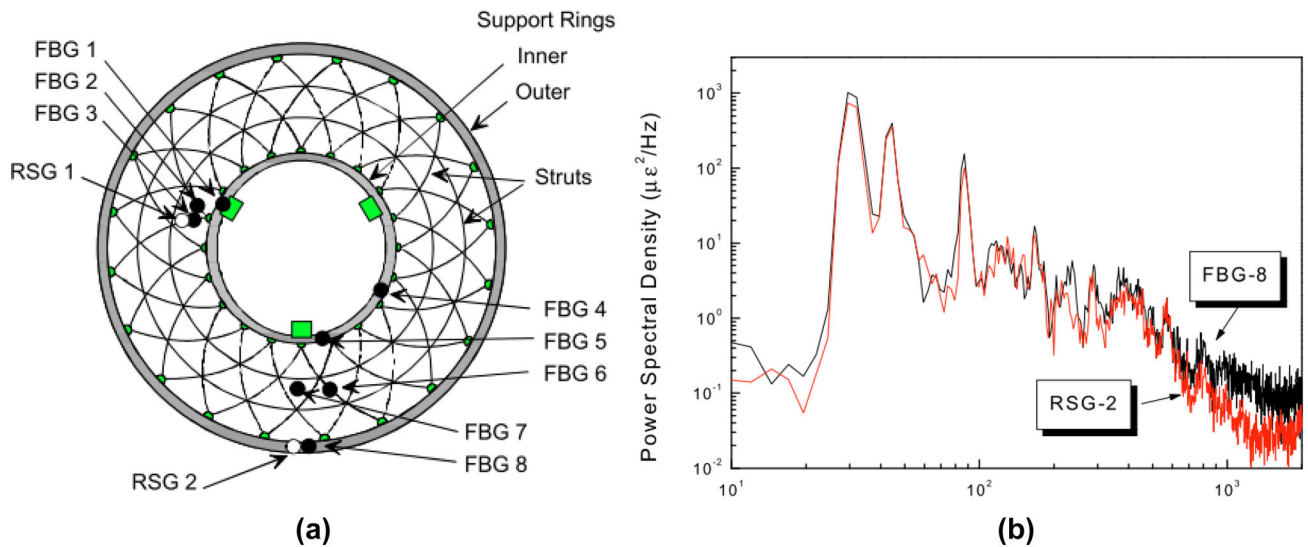


Fig. 14 **a** Schematic diagram of a lightweight antenna reflector structure showing locations of FBG and RSG strain sensors, **b** power spectral density against frequency using a 3.75 Hz sampling

bandwidth for RSG and FBG sensors. Reprinted with permission from Friebele et al. (1999). Copyright 1999, IOP Publishing Ltd

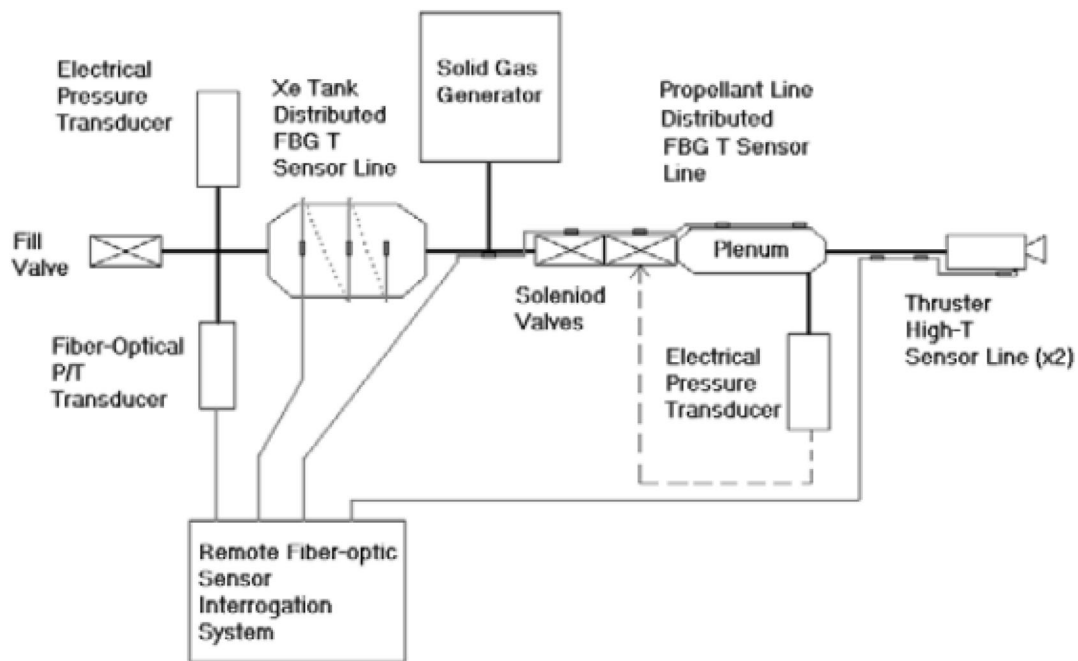


Fig. 15 Schematic of the fiber optic sensor demonstrator for the propulsion subsystem of PROBA II. Reprinted with permission from McKenzie and Karafolas (2005). Copyright 2005, Society of Photo-Optical Instrumentation Engineers (SPIE)

Temperature readings are required on more than 180 locations of Geosynchronous Telecommunication Satellite EUROSTAR3000 (EADS ASTRIUM’s satellite) for thermal mapping of the walls and floors of communication and service modules. The existing thermistor technology makes harnessing very heavy and time consuming. The multiplexing capability of FBG sensors reduces the weight of the harness and time for installation. The FBG sensors were

bonded on the satellite’s panel surface as embedment of sensors would affect the strength and manufacturing of the panels as well as prevent measurement spots on top or inside equipment boxes. Installation of FBG sensors yields a 74% mass decrease compared to the surface mounting of thermistors. Installation of FBG sensors decreases the overall cable length from over 350 m to less than 100 m) (Nannipieri et al. 2017).

Monitoring temperature during RF testing of array antenna

Measurement of temperature on certain elements of array type antenna, while being subjected to RF path particularly in aerospace systems is challenging. Temperature measurements are necessary for early detection of design problems. The metallic cables of conventional sensors like thermocouples and thermistors interfere with RF at certain frequencies. The immunity of Fiber optic sensors to electromagnetic interference (EMI) and its miniature size enables its deployment in small intricate gaps of antenna structures for thermal monitoring. FBG sensors can also be embedded without affecting the antenna operation. FBG temperature measurements in array antenna were demonstrated in two antenna samples: a stripline Wilkinson divider breadboard used for the center divider of the NAVANT (transmit antenna for GALILEO system) and a 1:3 Divider used in a NASA's Mars ROVER antenna. The presence of FBG sensors did not affect the performance of the antenna (Abad et al. 2017).

Thermal monitoring in electric propulsion subsystems

Temperature measurements in vital components of electric propulsion subsystems using conventional electrical sensors is hindered by the presence of high EM fields, free charged particles in the vacuum conditions of space environment. Three main parts in the ion engine propulsion system require thermal monitoring: (1) Ion engine thrusters require thermal monitoring on their walls as the impacts of accelerating ions degrade the lifetime of these engines. (2) High-Voltage Power supplies (HVPS) undergo a lot of heating during their operation, especially the high-voltage transformers. (3) High-voltage cables connecting HVPS to the engine require thermal mapping to monitor the cable performance. On a demonstrator, FBG temperature sensors were bonded on different locations to simulate the thruster's walls, the solenoids, and a high temperature spot. FBG sensors in S-shaped serial configuration to remove strain effects were used to measure temperature in the medium range (< 120 °C) while FBG sensors in terminal configuration were used for high temperature range (< 400 °C). The maximum temperature measured was limited by the material characteristic of optical fiber coating material (polyimide/Kapton). Overall, 19 FBG sensors were used on the demonstrator and signals were measured with a single interrogation unit. The FBG temperature sensors were tested at ambient pressure and thermal vacuum with high voltage, high magnetic field, plasma, and temperature gradient conditions and compared with thermocouple

readings. The FBG sensors were found to measure temperature better than thermocouple in the presence of high thermal gradient fields. FBG sensors also have a slightly faster response compared to thermocouples. Presence of EMI and electrical transients in high voltage conditions affects thermocouple measurements while FBG remains unaffected. FBG sensors are suitable for measuring temperature gradients in plasma and AC magnetic fields as well (Selwan and Ibrahim 2018).

Conclusions and future trends

In conclusion, we have reviewed the recent advances in applications of FBG sensor technology in aerospace engineering such as shock pressure sensing, structural health monitoring of spacecrafts and satellites, temperature monitoring of space structures, SHM of aircraft composites and diagnostics for aerodynamic ground test facilities. The theory and fabrication of FBG sensors have been discussed briefly. Owing to their small size, flexibility, and ability to withstand harsh environments FBG sensors can be used in shock sensing. FBG sensors have already been used in plate impact experiments to measure shock generated stress. Orientation of FBG with incoming shock wave is found to affect the sensitivity and response of the sensor. However, rugged sensor packaging and higher sampling rate of FBG data acquisition systems are required to deploy FBG sensors in field applications. FBG sensors and other fiber optic sensors have been used for strain, pressure and temperature monitoring in satellite and launcher subsystems, atmospheric entry vehicles, International Space Station (ISS), ground testing of antenna reflectors and solar sails, by various space organizations around the world. A hybrid combination of FBG sensor technology and other technologies in Reusable Launch Vehicles is being investigated by several space agencies. FBG sensors have been deployed in aircraft composite structures for monitoring the fabrication process, testing and structural health monitoring during their service. Real-time monitoring of evacuation process and detection of gas leaks using FBG sensors can be a valuable solution for the aerospace industry. However, further work is required in terms of design of fiber optic vacuum feedthroughs, sensitivity, and range of vacuum detection. Use of FBG sensors for simultaneous strain, temperature and pressure monitoring on test models in aerodynamic test facilities like hypersonic wind tunnels, shock tunnels has been demonstrated. With suitable packaging and the system implementation, FBG sensors can be used to measure other high-speed flow parameters as well. However, further research is needed in this area.

Declarations

Conflict of interest The authors declare that there are no conflicts of interest that have influenced the work reported in this paper.

References

- Abad S, Araújo FM, Ferreira LA, Pedersen F, Esteban MA, Mckenzie I, Karafolas N (2017) Applications of FBG sensors on telecom satellites. In: Proceedings of SPIE, vol 10565. <https://doi.org/10.1117/12.2309229>
- Aime LFJ, Verzeletti A, James SW, Tatam RP (2019) Optical fiber Bragg grating based pressure sensor using a composite diaphragm for pressure measurements. In: Proceedings of IEEE sensors 2019-October
- Barbarin Y, Lefrancois A, Magne S, Woirin K, Sinatti F et al (2016) Dynamic high pressure measurements using a fiber Bragg grating probe and an arrayed waveguide grating spectrometer. In: Interferometry XVIII, Aug, San Diego, United States, p 99600U. <https://doi.org/10.1117/12.2236651>, cea-01828507
- Barker LM, Hollenbach RE (1970) Shock-wave studies of PMMA, fused silica, and sapphire. *J Appl Phys* 41:4208. <https://doi.org/10.1063/1.1658439>
- Benterou J, Udd E (2012) Measuring detonation, deflagration and burn velocities with fiber-optic Bragg grating sensors. In: Advanced photonics Congress. OSA
- Benterou J, Udd E, Wilkins P, Roeske F, Roos E, Jackson D (2007) In situ continuous detonation velocity measurements using fiber-optic Bragg grating sensors. In: EuroPyro 2007, 34th international pyrotechnics seminar Beaune, France
- Benterou J, May C, Udd E, Mihailov SJ, Lu P (2011) High speed measurements using fiber-optic Bragg gratings. *Fiber Opt Sens Appl VIII* 8028:802808. <https://doi.org/10.1117/12.884703>
- Berkovic G, Shafir E, Zilberman S, Saadi Y, Ravid A, Fedotov Gefen A, Schweitzer Y (2018) Fiber Bragg gratings for dynamic high pressure measurements in shock wave research. In: Optics InfoBase conference papers part F98-B
- Chehura E, James SW, Lawson N, Garry KP, Tatam RP (2009) Pressure measurements on aircraft wing using phase-shifted fibre Bragg grating sensors. In: 20th International conference on optics fibre sensors, vol 7503, p 750334. <https://doi.org/10.1117/12.835469>
- Cheng LK, Smorenburg C, Scholtes JHG, van der Meer BJ (2001) Application of fiber optic interferometers for Cook-off measurements. In: Proceedings of SPIE, vol 4183
- Correia R, Chehura E, James SW, Tatam RP (2007) A pressure sensor based upon the transverse loading of a sub-section of an optical fibre Bragg grating. *Meas Sci Technol* 18:3103–3110. <https://doi.org/10.1088/0957-0233/18/10/S09>
- Cranch GA, Lunsford R, Grun J, Weaver J, Compton S, May M, Kostinski N (2013) Characterization of laser-driven shock waves in solids using a fiber optic pressure probe. *Appl Opt* 52:7791–7796
- Davison L (2008) Fundamentals of shock wave propagation in solids. Springer, Berlin. <https://doi.org/10.1007/978-3-540-74569-3>
- Deng X, Chen G, Peng Q, Li Z, Meng J, Liu J (2011) Research on the fiber Bragg grating sensor for the shock stress measurement. *Rev Sci Instrum* 82:103109. <https://doi.org/10.1063/1.3648123>
- Di Sante R (2015) Fibre optic sensors for structural health monitoring of aircraft composite structures: recent advances and applications. *Sensors* 15:18666–18713. <https://doi.org/10.3390/s150818666>
- Diaz V, Eaton N, Merillat S, Würth A, Ramusat G (2003) Reusable CFRP intertank structure for RLV stage. In: 54th International Astronautical Congress of the International Astronautical Federation (IAF), the International Academy of Astronautics and the International Institute of Space Law, vol 3, pp 1791–1801
- Ecke W, Grimm S, Latka I, Reutlinger A, Willsch R (2001) Optical fiber grating sensor network basing on high-reliable fibers and components for spacecraft health monitoring. In: Proceedings of SPIE, vol 4328. <https://doi.org/10.1117/12.435518>
- Floris I, Adam JM, Calderón PA, Sales S (2021) Fiber optic shape sensors: a comprehensive review. *Opt Lasers Eng* 139:106508. <https://doi.org/10.1016/j.optlaseng.2020.106508>
- Friebele EJ, Askins CG, Bosse AB, Kersey AD, Patrick HJ, Pogue WR, Putnam MA, Simon WR, Tasker FA, Vincent WS, Vohra ST (1999) Optical fiber sensors for spacecraft applications. *Smart Mater Struct* 8:813–838
- Friebele EJ, Askins CG, Miller GA, Peele JR, Wasserman LR (2004) Optical fiber sensors for spacecraft: applications and challenges. In: Proceedings of SPIE, vol 5554 (SPIE, Bellingham, WA, 2004). <https://doi.org/10.1117/12.562393>
- Goossens S, Berghmans F, Sharif Khodaei Z, Lambinet F, Karachalios E, Saenz-Castillo D, Geernaert T (2021) Practicalities of BVID detection on aerospace-grade CFRP materials with optical fibre sensors. *Compos Struct* 259:113243. <https://doi.org/10.1016/j.compstruct.2020.113243>
- Guru Prasad AS, Hegde GM, Asokan S (2010) Fiber Bragg grating sensors for real time monitoring of evacuation process. In: Proceedings of SPIE, vol 7522. <https://doi.org/10.1117/12.852743>
- Guru Prasad AS, Sharath U, Nagarjun V, Hegde GM, Asokan S (2013) Measurement of temperature and pressure on the surface of a blunt cone using FBG sensor in hypersonic wind tunnel. *Meas Sci Technol* 24:095302. <https://doi.org/10.1088/0957-0233/24/9/095302>
- Hegde GM, Asundi AK (2003) Performance of a fiber optic polarimetric sensor in health monitoring of different smart structures. In: SPIE, smart materials, structures, and systems, vol 5062, pp 736–740
- Hegde G, Asundi A (2006) Performance analysis of all-fiber polarimetric strain sensor for composites structural health monitoring. *NDT E Int* 39(4):320–327
- Hegde G, Prasad MVN, Asokan S (2021) Temperature compensated diaphragm based fiber Bragg grating (FBG) sensor for high pressure measurement for space applications. *Microelectron Eng* 248:111615
- Hill KO, Fujii Y, Johnson DC, Kawasaki BS (1978) Photosensitivity in optical fiber waveguides: application to reflection filter fabrication. *Appl Phys Lett* 32:647–649
- Hill KO et al (1993) Bragg gratings fabricated in monomode photosensitive optical fiber by UV exposure thorough a phase-mask. *Appl Phys Lett* 62(10):1035–1037
- Hsu C-Y, Chiang C-C, Hsieh T-S, Chen T-H, Chen Y-H (2020) A study of strain measurement in cylindrical shells subjected to underwater shock loading using FBG sensors. *Optik (stuttgart)* 217:164701. <https://doi.org/10.1016/j.ijleo.2020.164701>
- Jinachandran S, Rajan G (2021) Fibre Bragg grating based acoustic emission measurement system for structural health monitoring applications. *Materials* 14:897. <https://doi.org/10.3390/ma14040897>
- Jitschin W, Ludwig S (2004) Dynamical behavior of the Pirani sensor. *Vacuum* 75:169–176. <https://doi.org/10.1016/j.vacuum.2004.02.002>
- Jukes TN, Segawa T, Furutani H (2012) Active flow separation control on a NACA 4418 using DBD vortex generators and FBG sensors. In: 50th AIAA Aerospace sciences meeting including the new horizons forum and aerospace exposition, pp 1–2

- Kabashima S, Ozaki T, Takeda N (2001) Structural health monitoring using FBG sensors in space environment. In: Proceedings of SPIE, vol 4332. <https://doi.org/10.1117/12.429644>
- Kahandawa GC, Epaarachchi J, Wang H, Lau KT (2012) Use of FBG sensors for SHM in aerospace structures. *Photonic Sens* 2:203–214. <https://doi.org/10.1007/s13320-012-0065-4>
- Kashyap R (1999) *Fiber Bragg gratings*. Academic Press, San Diego
- Kishore CM, Srihari GK, Rudresh C, Ravi V, Karale SP, Padbidri S, Jagadeesh G, Vasudevan B (2005) Aerodynamic load measurements at hypersonic speeds using internally mounted fiber-optic balance system. In: 21st International Congress on instrumentation in aerospace simulation facilities (Japan), pp 119–122
- Kuznetsov AB, Serieznov AN, Lukyanov AV, Bragin AA (2021) Measuring deformation, temperature, vibration and acoustic emission signals of aircraft structures using fiber optical sensors. *AIP Conf Proc* 2351:030010. <https://doi.org/10.1063/5.0053873>
- Latka I, Ecke W, Höfer B, Chojetzki C, Reutlinger A (2004) Fiber optic sensors for the monitoring of cryogenic spacecraft tank structures. In: Proceedings of SPIE, vol 5579 (SPIE, Bellingham, WA). <https://doi.org/10.1117/12.567353>
- Lawson NJ, Correia R, James SW, Partridge M, Staines SE, Gautrey JE, Garry KP, Holt JC, Tatam RP (2016) Development and application of optical fibre strain and pressure sensors for in-flight measurements. *Meas Sci Technol* 27:104001. <https://doi.org/10.1088/0957-0233/27/10/104001>
- Lee KW, Peiyi AC, Chan F, Ho J, Shelly J, Asundi AK, Hegde GM (2003) Sensitivity analysis of all fibers in polarimetric fiber optic sensor for structural health monitoring of composites. In: SPIE, nondestructive evaluation and health monitoring of aerospace materials and composites II, vol 5046, pp 185–190
- Magne S, Lefrançois A, Luc J, Laffont G, Ferdinand P (2013) Real-time, distributed measurement of detonation velocities inside high explosives with the help of chirped fiber Bragg gratings. In: Proceedings of SPIE, vol 8794. <https://doi.org/10.1117/12.2025986>
- Mckenzie I, Karafolas N (2005) Fiber optic sensing in space structures: the experience of the European Space Agency. In: Proceedings of SPIE, vol 5855 (SPIE, Bellingham, WA, 2005). <https://doi.org/10.1117/12.623988>
- Meltz G, Morey WW (1991) Bragg grating formation and germanosilicate fiber photosensitivity. *Proc SPIE* 1516:185–199
- Meltz G, Morey WW, Glenn WH (1989) Formation of Bragg gratings in optical fibers by a transverse holographic method. *Opt Lett* 14:823–825
- Mihailov SJ (2012) Fiber Bragg grating sensors for harsh environments. *Sensors* 12:1898–1918. <https://doi.org/10.3390/s120201898>
- Nannipieri P, Meoni G, Nesti F, Mancini E, Celi F, Quadrelli L, Ferrato E, Guardati P, Baronti F, Fanucci L, Signorini A, Nannipieri T (2017) Application of FBG sensors to temperature measurement on board of the REXUS 22 sounding rocket in the framework of the U-PHOS project. In: 4th IEEE international workshop on metrology for AeroSpace, MetroAeroSpace (2017)—proceedings, pp 462–467
- Nicolas MJ, Sullivan RW, Richards WL (2016) Large scale applications using FBG sensors: determination of in-flight loads and shape of a composite aircraft wing. *Aerospace* 3:18. <https://doi.org/10.3390/aerospace3030018>
- Othonos A (1997) Fiber Bragg gratings. *Rev Sci Instrum* 68(12):4309–4341
- Othonos A, Kalli K (1999) *Fiber Bragg gratings: fundamentals and applications in telecommunications and sensing*. Artech House, Norwood
- Prinse WC, van der Meer BJ, Scholtes JHG, Cheng LK, Smorenburg C, van Bree JLMJ, Bouma RHB (2001) Development of fibre optic sensors at TNO for explosion and shock wave measurements. In: Proceedings of SPIE, vol 4183
- Qiu H, Min F, Yang Y (2020) Fiber optic sensing technologies potentially applicable for hypersonic wind tunnel harsh environments. *Adv Aerodyn* 2:1–22. <https://doi.org/10.1186/s42774-020-00033-y>
- Ravid A, Shafir E, Zilberman S, Berkovic G, Glam B, Appelbaum G, Gefen AF (2014) Fibre Bragg grating sensor for shock wave diagnostics. *J Phys Conf Ser* 500:142029. <https://doi.org/10.1088/1742-6596/500/14/142029>
- Renson LFP (2003) Health monitoring system for future reusable launcher: from operational aspects to mission risk management impacts. *Smart Nondestruct Eval Heal Monit Struct Biol Syst II* 5047:96
- Rocha H, Semprinoschnig C, Nunes JP (2021) Sensors for process and structural health monitoring of aerospace composites: a review. *Eng Struct* 237:112231. <https://doi.org/10.1016/j.engstruct.2021.112231>
- Rodriguez G, Gilbertson SM (2017) Ultrafast fiber Bragg grating interrogation for sensing in detonation and shock wave experiments. *Sensors* 17:248. <https://doi.org/10.3390/s17020248>
- Rodriguez G, Sandberg RL, Jackson SI, Dattelbaum DM, Vincent SW, McCulloch Q, Martinez RM, Gilbertson SM, Udd E (2013) Fiber Bragg grating sensing of detonation and shock experiments at Los Alamos National Laboratory. *Fiber Opt Sens Appl X* 8722:872204. <https://doi.org/10.1117/12.2015188>
- Rodriguez G, Sandberg RL, Lalone BM, Marshall BR, Grover M, Stevens G, Udd E (2014) High pressure sensing and dynamics using high speed fiber Bragg grating interrogation systems. *Fiber Opt Sensors Appl XI* 9098:90980C. <https://doi.org/10.1117/12.2054600>
- Sandberg RL, Rodriguez G, Gibson LL, Dattelbaum DM, Stevens GD, Grover M, Lalone BM, Udd E (2014) Embedded optical probes for simultaneous pressure and temperature measurement of materials in extreme conditions. *J Phys Conf Ser* 500:142031. <https://doi.org/10.1088/1742-6596/500/14/142031>
- Segawa T, Abe H, Kikushima Y, Yoshida H, Mizunuma H (2003) Measurement of turbulent skin frictional drag using a fiber Bragg grating system. In: 41st Aerospace science meetings and exhibit, pp 1–8
- Selwan MF, Ibrahim K (2018) Fiber sensing for space applications. In: Conference ECSSMET 2018 at ESTEC, Netherlands
- Setchell RE (1979) Index of refraction of shock-compressed fused silica and sapphire. *J Appl Phys* 50:8186. <https://doi.org/10.1063/1.325959>
- Shafir E, Berkovic G, Fedotov-Gefen A, Ravid A, Zilberman S, Schweitzer Y (2017) Shock-wave measurements with fiber Bragg gratings. In: Conference on lasers electro-optics Pacific Rim, CLEO-PR January, pp 1–4
- Sriram R, Ram SN, Hegde GM, Nayak MM, Jagadeesh G (2015) Shock tunnel measurements of surface pressures in shock induced separated flow field using MEMS sensor array. *Meas Sci Technol* 26:95301
- Udd E (2011) Sensing high speed phenomena using fiber gratings and the Sagnac interferometer. In: Proceedings of SPIE, vol 7753. <https://doi.org/10.1117/12.884889>
- Udd E (2014) High speed fiber grating pressure sensors. In: Proceedings of SPIE, vol 9098. <https://doi.org/10.1117/12.2054439>
- Udd E, Benterou J (2012) Improvements to high-speed monitoring of events in extreme environments using fiber Bragg grating sensors. In: Proceedings of SPIE, vol 8370. SPIE. <https://doi.org/10.1117/12.915726>
- Van't Hof PG, Cheng LK, Scholtes JHG, Prinse WC (2007) Dynamic pressure measurement of shock waves in explosives by means of

a fiber Bragg grating sensor. In: Proceedings of SPIE, vol 6279, p 62791Y-1. <https://doi.org/10.1117/12.725258>

Yu Y, Liu B, Xia F (2022) Design optimization of sensitivity-enhanced structure for fiber Bragg grating acoustic emission sensor based on additive manufacturing. Sensors 22:416. <https://doi.org/10.3390/s22020416>

Publisher's Note Springer Nature remains neutral with regard to jurisdictional claims in published maps and institutional affiliations.